

Discussion of “Generalized Head-Discharge Equation for Flow over Sharp-Crested Inclined Inverted V-Notch Weir” by M. N. Shesha Prakash and A. V. Shivapur

July/August 2004, Vol. 130, No. 4, pp. 325–330.
DOI: 10.1061/(ASCE)0733-9437(2004)130:4(325)

A. Burcu Altan-Sakarya¹

¹Assistant Professor, Civil Engineering Dept., Middle East Technical Univ., Ankara, Turkey. E-mail: burcuas@metu.edu.tr

The authors obtained a linear head-discharge equation for sharp-crested inclined inverted V-notch (IIVN) weirs after performing several experimental studies for different inclination angles. Even though the given linear relationship is very convenient to use, some important remarks need to be clarified for future users of these kinds of weirs.

Initially, the authors decompose the total discharge into x and y components by taking the vertical and horizontal projection of the IIVN weir [Eq. (1) of the paper]. It is not clear why the x component of the discharge, q_x , is assumed to have the exact same formulation as the discharge that would pass from a normal (no inclination with vertical) weir, q_n [Eq. (2) of the paper]. Furthermore, no explanation is provided for assuming the y component of the discharge, q_y , as the tangent of the inclination angle, $\tan \alpha$, multiplied by q_x [Eq. (3) of the paper]. The authors then use Eqs. (1) to (3) to obtain Eq. (4), which defines the total discharge through the inclined weir as the discharge passing through the normal weir, q_n , and an additional amount of discharge. This additional discharge term is initially assumed to be equal to $\tan \alpha q_n$ and is afterwards updated by including β . Assuming that Eq. (4) represents the total discharge through the inclined weir is understandable, but no explanation is given for assuming that $q_x = q_n$ and that $q_y = \tan \alpha q_x$. In fact, in deriving the total discharge, there is no need to break the total discharge down into x and y components. Writing Eq. (4) directly is sufficient and logical. Also, the limits of head above crest, h , for these equations are given as 0 to the height of the weir, d . For the inclined weir, it is clear that the weir will be flowing full and will not act as a weir when the head, h , exceeds $d \cos \alpha$ (or a value a little bit more than $d \cos \alpha$ because of the decrease in head at the weir location). Hence, the given limits of the equations are not realistic and should be 0 to $d \cos \alpha$ instead of 0 to d . The writer assumes that an error has occurred in Fig. 1 of the paper. The height of the weir in Fig. 1(a) is shown as d ; hence, in Fig. 1(b), the vertical distance should be $d \cos \alpha$ instead of d . This thought is also verified by the experimental data, in which the maximum h value studied for $\alpha = 60^\circ$ is around 0.09 m—a value close to $d \cos \alpha$ —instead of 0.1732 m, which is the value of d for the given weir. Also, in Fig. 1(a), to be consistent with the given equations, all the angles should be θ instead of $\theta/2$. Otherwise, all the equations should be corrected as $\tan(\theta/2)$ instead of $\tan \theta$.

The authors explained an optimization procedure to determine the maximum linearity range. However, throughout the paper, the pre-fixed maximum allowable value of the relative percentage deviation of the linear fit, E , is not provided. Without this value, the proposed methodology cannot work. The discussor calculates that it could be $\pm 1.5\%$, as in Keshava Murty and Giridhar (1989). However, with $E = \pm 1.5\%$, the proposed linear equation cuts the Q_D curve when the value of the nondimensional head, H , is from 0.64 to 0.68. Unfortunately, H_2 , H_3 , and E are not given in the paper; hence, this point remains unclear.

Keshava Murty and Giridhar (1989) suggested the value of the slope of the line to be 0.4481, not 0.448, as in Table 1 of the paper. With the proposed new methodology, the authors obtained a similar equation but extended the limits of the linearity range. A misprint exists in Eq. (20). The power of H_2 and H_3 should be $5/2$ instead of $1/2$.

Fig. 3 in the paper gives the variation of nondimensional theoretical discharge versus nondimensional head (note that an error has occurred, and all the discharges must be multiplied by 10 to arrive at the correct values of the discharges). As shown in the graph, the head varies between 0 and 1 for all the inclination angles. As previously stated, the upper limit of the head on the weir should be $d \cos \alpha$ instead of d . Hence, the graph that considers the upper bounds of H is shown in Fig. 1. In this figure, the relationship between nondimensional discharge and head is the relationship that was given by the authors in Eq. (23) in the paper. The correct upper bounds are used in Fig. 1, where, for example, H cannot be equal to 1 when $\alpha = 60^\circ$, since the weir will be flowing full. Then after experimental studies, the authors suggested including β , and the new form of the equation is

$$Q_e = 0.448(H - 0.0817)(1 + \beta \tan \alpha) \quad (1)$$

Fig. 2 shows the relationship between the estimated nondimensional discharge and the nondimensional head by using Eq. (1). For example, when $H = 0.5$, the nondimensional discharge passing through the normal weir is 0.187 and 0.228 for $\alpha = 60^\circ$. There

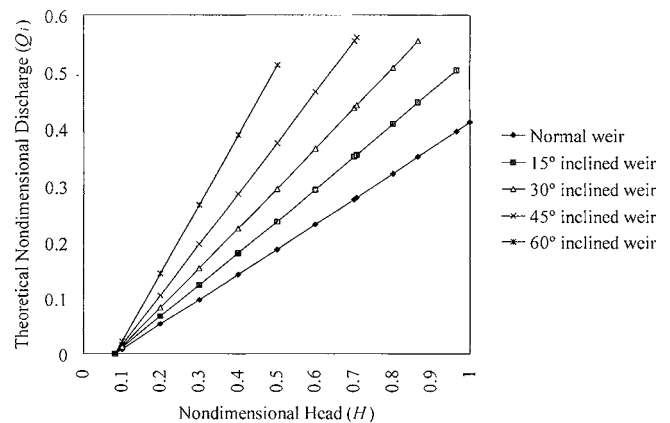


Fig. 1. Variation of theoretical nondimensional discharge versus nondimensional head

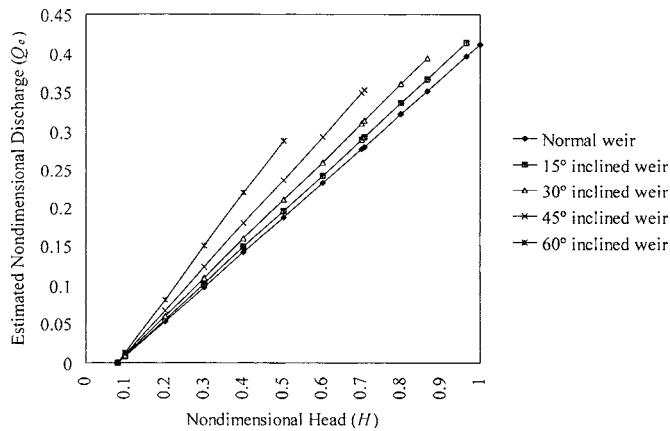


Fig. 2. Variation of estimated nondimensional discharge versus nondimensional head

is a 53.7% increase in the discharge relative to the normal weir (26.0, 12.1, and 4.2% increases occur when $\alpha=45$, 30, and 15° , respectively; the increase in the discharge is higher than the values provided in Table 3 in the paper). In fact, there will be a $\beta \tan \alpha$ increase for every weir [β is given in Eq. (26) in the paper]. But there is a different upper limit of H for every weir, and it is slightly higher than $\cos \alpha$. Hence, for lower heads, having the weir inclined might increase the discharge up to 53.7% for $\alpha=60^\circ$. This outcome is the advantage of the inclined weirs. However, the limit of H also limits the discharge. The upper limit on nondimensional discharge for a 60° inclined weir is 0.288, whereas 0.411 is the discharge passing through the weir for $H=1$ when $\alpha=0$. Fig. 8 in the paper also shows this limit. When $\alpha=60^\circ$, the experimental studies are made up to a head of around 0.08 m (0.0957 m is reported in Table 2 but not shown in Fig. 8). The theoretical limit on h is $d \cos \alpha = w \tan \theta \cos \alpha = 0.087$ m ($\theta=60^\circ$ and $\alpha=60^\circ$). After this height, the weir will no longer be a weir. This problem is a very interesting one, and the relation between h and Q when the upper limit on h exceeds on weir can be the subject of a future study.

References

- Keshava Murthy, K., and Giridhar, D. P. (1989). "Inverted V-notch: A practical proportional weir." *J. Irrig. Drain. Eng.*, 115(6), 1035–1050.

Closure to "Generalized Head-Discharge Equation for Flow over Sharp-Crested Inclined Inverted V-Notch Weir" by M. N. Shesha Prakash and A. V. Shivapur

July/August 2004, Vol. 130, No. 4, pp. 325–330.
DOI: 10.1061/(ASCE)0733-9437(2004)130:4(325)

M. N. Shesha Prakash¹ and A. V. Shivapur²

¹Professor, Civil Engineering Dept., Jawaharlal Nehru National College of Engineering, Shimoga-577 204, India.

²Assistant Professor, Civil Engineering Dept., S.D.M. College of Engineering and Technology, Dharwad-580 002, India.

The writers appreciate the discussor's interest in the paper and thank him for the comments. The following is the writers' response to the discussor's comments.

- Eq. (2) and Eq. (3) have been obtained by considering discharge through the inclined notch weir as the combination of discharge through the vertical projection and the horizontal projection (as an orifice), respectively. The detailed derivation could not be given because of the length constraint of the paper. However, readers can refer to the papers published by Shesha Prakash and Shivapur (2004 a,b), in which a similar approach is followed for developing the discharge equation. Eq. (4) is the sum of Eq. (2) and Eq. (3). Therefore, the equation obtained after simplification is $(1 + \tan \alpha)$ times the discharge through the normal weir.
- While deriving the general discharge equation, Eq. (4), the writers consider resolving the inclined portion into vertical and horizontal portions as an approach. However, Eq. (4) can also be written as $q_n(1 + \beta)$, where β can be a factor, which takes care of extra discharge attributable to the inclination's being given in the direction of flow. In that case, β has to be expressed in terms of inclination (α) in radians.
- In Fig. 1, d has to be read as the height of IIVN, i.e., the maximum range of head for a given inclined notch-weir. Therefore, the vertical distance is d , not $d \cos \alpha$. The maximum range of head for $\alpha=60^\circ$ is 0.0866 m. Although the experiments were carried out for the range of variables mentioned in Table 2, only those values that are within the linearity range, as obtained by the optimization procedure developed herein, are used. The maximum head used for analysis in the case of $\alpha=60^\circ$ is 0.0812 m, which is very close to the maximum linearity range 0.0817 m (i.e., 0.943 times 0.0866 m) and is evident from Fig. 5 and Fig. 8 in the paper. The maximum range of head for a normal weir is 0.1732 m. The angle ($\theta/2$) in the equation developed by the writers is correct.
- The writers thank the discussor about not mentioning the pre-fixed allowable percentage error in the paper. The writers agree with the comments of the discussor and would like to clarify that the relative percentage error in the proposed methodology in the paper has been taken as $\pm 1.5\%$. The interest of the optimization technique is to determine the maximum linearity range; hence, the values H_2 and H_3 have no significance. Therefore, H_2 and H_3 values were not given.
- The value of the slope of the line, as obtained by the writers (i.e., 0.448091), matches very closely with the value obtained by Keshava Murthy and Giridhar (1989) as 0.4481. Therefore, the writers restricted the preceding value to a third decimal place as 0.448. In view of the exact solution to the linearity range by the newly developed optimization procedure, the linearity is $0.943d$, as compared to $0.940d$ obtained by Keshava Murthy and Giridhar (1989). The powers of H_2 and H_3 in Eq. (20) are correct.
- The writers agree with the discussor that the nondimensional discharge values in Fig. 3 in the paper have to be read by multiplying by 10. The writers regret the incorrect depiction of values.
- The percentage increase in relative discharge with respect to normal with α (Table 3) has been obtained as the average percentage increase in estimated discharge with volumetric

discharge measurement for various heads. However, the writers agree with the discussor that the discharge increases by $\beta \tan \alpha$ for inclined weirs, as compared with a normal weir. Therefore, the increase in discharge in Table 3 can be read as 53.71, 25.96, 12.07, and 4.25% for $\alpha=60, 45, 30,$ and 15° , respectively.

8. When the head exceeds d , the weir will flow full and will act as an orifice. The study of such an inclined orifice is quite interesting, and the writers are working out the advantages of such an orifice and will publish this material at a later date.

Shivapur A. V. wishes to thank AICTE for providing financial assistance under R&D Project (0821/RID/NPRO/078/2/3 dated May 19, 2003) to carry out this study.

Erratum

On page 330 of the paper, the notation D has to be taken as d .

References

- Keshava Murty, K., and Giridhar, D. P. (1989). "Inverted V-notch: A practical proportional weir." *J. Irrig. Drain. Eng.*, 115(6), 1035–1050.
- Shesha Prakash, M. N., and Shivapur, A. V. (2004a). "Use of inclined rectangular weir for flow measurement with lesser afflux." *J. Appl. Hydrol.*, 17(1), 59–68.
- Shesha Prakash, M. N., and Shivapur, A. V. (2004b). "Characteristics for flow through inclined triangular notch-weir." *J. Hydrol.*, 27(1–2), 43–53.

Discussion of "Comparative Analysis of Hydraulic Calculation Methods in Design of Microirrigation Laterals" by Gürol Yildirim and Necati Ağralıoğlu

May/June 2004, Vol. 130, No. 3, pp. 201–217.

DOI: 10.1061/(ASCE)0733-9437(2004)130:3(201)

Giuseppe Provenzano¹ and Guillermo Palau-Salvador²

¹Researcher, Dept. di Ingegneria e Tecnologie Agro-Forestali, Sezione Idraulica, Univ. di Palermo, Viale delle Scienze 12, 90128 Palermo, Italy. E-mail: gproven@unipa.it

²Assistant Professor, Dept. de Ingenieria Rural y Agroalimentaria, Unidad Hidráulica, Univ. Politécnica de Valencia, Camino de Vera s/n, 46022 Valencia, Spain. E-mail: guipasal@agf.upv.edu

The discussors appreciate the efforts of the authors to present a comparative analysis of hydraulic calculation methods in designing microirrigation laterals. The problem has practical relevance, since adequate analysis of trickle lateral hydraulics allows proper design and evaluation of existing drip irrigation systems.

In the paper, a comparison between seven different procedures for hydraulic calculations and design of drip laterals was carried out in order to indicate evidence the differences and distinguish limits in their application for various combinations of design parameters.

As suggested by Wu (1997), the accurate design of a drip lateral line should be finalized to achieve a relatively high value of the field emission coefficient. This coefficient is affected by the manufacturer's variation, emitter spacings, grouping of emitters per plant, plugging, and soil hydraulic characteristics. It is therefore necessary to consider, as a factor that affects the emission uniformity, the emitter discharge variations along the lateral, depending on both the elevation changes and the head loss along the lines, as well as the manufacturing variability, clogging, and water temperature.

Several studies have been published with the aim of evaluating the pressure-head distribution along the laterals, the emitter discharge, and the consequent emission uniformity coefficient (EU), expressed as Christiansen's uniformity coefficient (UC) and the lower-quarter distribution uniformity coefficient (DU), which is defined as

$$UC = 1 - \frac{1}{Nq_{av}} \sum_{i=1}^N |q_i - q_{av}| \quad (1a)$$

$$DU = \frac{4}{Nq_{av}} \sum_{i=1}^{N/4} (q_{low})_i \quad (1b)$$

where N =number of emitters; and q_i , q_{av} , and $(q_{low})_i$ (L/h) =discharge at emitter i , the average along the lateral, and the discharge of the lower-quarter emitters, respectively. Bralts et al. (1987) proposed to evaluate the performance of drip irrigation units by the emitter flow variation (V_{HM}), expressed as a function of the effective pressure-head variation at the emitters, V_H , and the emitter's manufacturer's variation coefficient, V_M , as indicated in Eq. (55) of the discussed paper.

The most accurate solution for designing a drip lateral can be reached by the forward-step-calculation method (FSM), which allows proper evaluation of head losses along the laterals and takes into account local losses caused by the presence of the emitters (Al Amoud 1995; Provenzano et al. 2005).

Accurate evaluation of head losses along drip laterals is therefore necessary because drip laterals strongly affect the available head at emitter nozzles and consequently affect the flow rates when conventional noncompensating emitters are used. Many authors (Jeppson 1982; Bagarello and Pumo 1992; Al Amoud 1995; Juana et al. 2002; Valiantzas 2002; Palau Salvador et al. 2004) highlighted the importance of considering local losses in drip laterals where a high number of emitters are installed. The emitter connections modify the flow streamlines, introducing additional turbulence and consequently local head losses, sometimes called minor losses, which must be added to the friction losses occurring in the pipe to determine the total losses along the laterals (Jeppson 1982). Although the head loss produced by each emitter is usually small, the total amount of minor losses in a lateral line can become significant, since emitter spacing can be very small and since many emitters can be inserted along the lateral (Howell and Barinas 1980; Al Amoud 1995; Bagarello et al. 1997).

The protrusions of on-line emitter barbs into the flow cause contraction of the flow streamlines and subsequent enlargement. In-line or integrated emitters determine the contraction of the flow paths at the upstream connection and the expansion of the flow paths immediately downstream from the emitters, because they usually have a smaller diameter than the pipe. Hence, higher frictional head losses, caused by the lower cross-section area, must therefore be considered (Bagarello and Pumo 1992). Moreover, computational fluid dynamics techniques (CFD) have

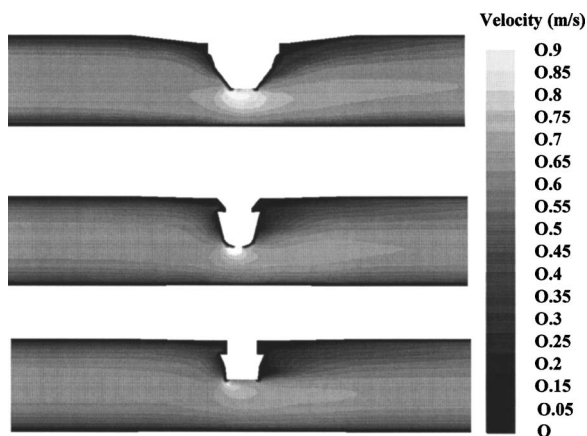


Fig. 1. Velocity contours for three different on-line emitters for a flow rate in the pipe equal to 250 L/h

been used to analyze and simulate different turbulent flows through valves, pumps, nozzles, or other hydraulic devices (Veersteg and Malalasekera 1995). CFD codes solve the main equations of fluid dynamics (the conservation of mass, the momentum equation,

and the energy equation) to obtain average values of pressure and velocity in the control volumes defined by using a grid. Fig. 1 shows the velocity contours around three different on-line emitters installed in a pipe having an internal diameter equal to 13.21 mm, obtained in the symmetry plane containing the emitter connection for a flow rate at the upstream end of the pipe equal to 250 L/h, by using CFD technique. Moreover, the detailed shape of the velocity field, obtained for the first emitter and represented by means of vectors, is shown in Fig. 2.

Experimental investigations performed by using laterals with both on-line emitters and integrated in-line emitters showed that the α coefficient, which expresses local losses as a fraction of the kinetic head (De Marchi 1954), can practically be considered independent of the Reynolds number but are dependent on the ratio between the pipe section A_i and the flow cross-section area A_g , where the emitter is located; neglecting the morphology of the connection allows estimation of values of α as a function of a simple parameter expressing the connection geometry, using the empirical approach suggested by Bagarello et al. (1997) for laterals with on-line emitters and by Provenzano and Pumo (2004) for laterals with coextruded in-line emitters.

Comparing the α values obtained by Bagarello et al. (1997) for on-line emitters and those of Provenzano and Pumo (2004) for integrated emitters gave the result that in the range $1.00 < A_i/A_g < 1.20$, the α values determined for on-line emitters (α_{on}), were almost coincident with those obtained for integrated in-line emitters (α_{in}) and variable in the range $0 < \alpha < 0.20$. In the range $1.20 < A_i/A_g < 1.44$, the differences between α_{in} and α_{on} increased with the ratio A_i/A_g , with α values variable between 0.20 and 1.39 for in-line coextruded emitters and between 0.20 and 0.58 for on-line emitters, respectively (Provenzano 2004). For the lowest A_i/A_g values, disturbance of the main flow should be limited and the flow consequently does not separate from the walls behind the emitter. The higher the A_i/A_g ratio, the more significant the disturbance of the main flow attributable to the emitters. The complete separation of the streamlines from the boundary, behind the in-line emitters, could

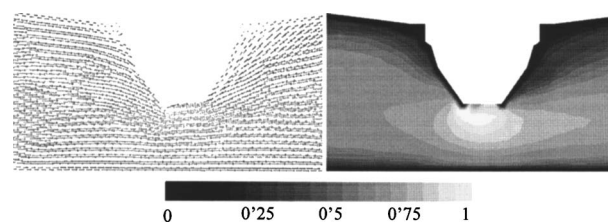


Fig. 2. Particulars of the velocity field around the first emitter shown in Fig. 1 (units in m/s)

be responsible for the higher head losses observed, whereas in the on-line emitters with an equal A_i/A_g ratio, the separation of the streamlines can be related to only a fraction of the cross-section area.

The result fits with that found by Howell and Barinas (1980), who, on the basis of experiments carried out with five different on-line models and one in-line emitter model, concluded that in-line emitters had significantly larger pressure losses than on-line emitters.

Recently Palau-Salvador et al. (2004) proposed a different approach, which was based on the CFD techniques, for to evaluating local losses attributable to on-line emitter connections. Local losses produced by two different models were simulated on the basis of the turbulence analysis around the emitter connection. The Reynolds stress model was used to obtain a simulation of the local losses produced by the protrusion area of the emitter. The model represented accurately the log-law velocity distribution near the wall (Schlichting 1979) and the drop pressure obtained from the experimental tests.

However, the different methodologies proposed in the discussed paper, except for the forward step method (FSM) do not take into account the local losses attributable to the emitter connections. Some of the proposed formulations, because of the introduced assumptions and simplifications, have to be considered as approximate solutions of the problem. Moreover, as indicated in Table 2 of the paper, some of the proposed methodologies must be used only when the exponent γ of the pressure-head relationship is equal to 0.5, as in the case of the Runge-Kutta numerical method (RKM) and the simplified analytical approach (SAA), or 1.0 for the constant discharge method (CDM) and variable discharge method (VDM).

As suggested by different authors (Christiansen 1942; Zayani et al. 2001), a first approximate evaluation of total losses along a drip lateral can be obtained by assuming that the outlet discharge for all the emitters installed along the lateral is constant. For noncompensating emitters, this hypothesis is actually not verified because the outlet discharge is spatially varied according to the pressure head distribution along the lateral. This assumption could be considered a good approximation when outflow variation Δq , obtained by dividing the difference between the maximum (q_{max}) and minimum (q_{min}) emitter outflows by the mean value (q_{av}), is less than 10% as a consequence of the limited pressure-head variations (Wu 1997; Vallesquino and Luque Escamilla 2002).

Other simplified approaches for hydraulic calculations of drip laterals were recently proposed with the aim of avoiding the tedious calculations consequent to the FSM, as well as avoiding the use of computers such as in underdeveloped countries or for didactic applications (Vallesquino and Luque Escamilla 2002; Provenzano et al. 2004). Those approaches also allow a first

approximate evaluation of the design's unknown variables. When on-line emitters are installed along a lateral, choosing pipe diameter and length as design variables is possible to obtain a relatively high value of EU. When the pipe diameter is a priori known, such as in the case of in-line or integrated emitters, only the lateral length has to be determined.

Afterward, the approximate values for the design variables (pipe length and diameter) determined by a simplified procedure, can be used with the FSM to obtain the correct value of EU.

Under the assumption of constant emitter flow rate, Provenzano et al. (2004) proposed a simplified procedure to evaluate the friction and the local losses along a lateral attributable to the emitter.

The total friction losses, h_f , between the first and the N th emitter of a lateral can be calculated as the sum of the single friction losses between consecutive emitters

$$h_f = \sum_{i=1}^{N-1} h_{fi} = k * v^{0.25} \frac{q_{av}^{1.75}}{D^{4.75}} S \sum_{i=1}^{N-1} (i)^{1.75} \quad (2)$$

where k =constant; v (L^2T^{-1})=cinematic water viscosity; q_{av} (L^3T^{-1})=average discharge of a single emitter; D (L)=inside pipe diameter; and S (L)=emitter spacing. Eq. (2) was obtained by considering that the friction losses can be evaluated by using the Darcy-Weisbach equation. The value of the constant k is equal to 0.0246 if the friction factor is obtained by using the Blasius equation and 0.0235 if it is calculated according to the following relationship (Bagarello et al. 1995):

$$f = 0.302 \Re^{-0.25} \quad (3)$$

experimentally obtained in the range $2,000 < \Re < 36,000$ for small-diameter polyethylene pipes (PE).

Since each local loss attributable to the emitter connection, h_{Li} , is expressed as a fraction α of the kinetic head, the total local losses along a lateral, h_L in which N emitters are installed can be calculated as sum of single local losses, h_{Li} , at the generic emitter:

$$h_L = \sum_{i=1}^{N-1} h_{Li} = \alpha \frac{8}{g \pi^2} \frac{q_{av}^2}{D^4} \sum_{i=1}^{N-1} i^2 \quad (4)$$

considering outlet flow rate constant and equal to the nominal value, q_{av} .

Eqs. (2) and (4) can be used to calculate friction and local losses between the first and the last emitter of a lateral, for which the α coefficient and mean emitter flow rate are known.

Numerical Examples

In the discussed paper, numerical examples were proposed by using the different design methodologies to evaluate the inlet pressure, the lateral length, and the internal diameter for different combinations of the lateral slope and the exponent y of the flow rate–pressure head relationship, which was assumed to be variable between 0.2 and 1.0.

The higher the exponent y , the more noticeable is the result of the differences of the emitters' flow rate attributable to pressure head variations. The value of y equal to 0.5 is typical for short path emitters characterized by turbulent flow conditions, whereas y equal to 1.0 is generally related to laminar flow conditions in long path emitters.

In all the proposed examples, the local losses attributable to the emitter connections were not taken into account. To evaluate the weight of local losses attributable to the emitter connections, some of the examples are repropose by considering different emitter models that are characterized by known values of the α coefficient.

The FSM, which is characterized by the highest level of accuracy, was used to evaluate friction and local losses as well as the emission uniformity coefficients UC and DU. A computer spreadsheet that reproduces the procedure was devised by considering the data indicated in the discussed paper for determining inlet pressure head and by considering the emitters characterized by an exponent y equal to 0.5 (Case A) and equal to 1.0 (Case B). A lateral length of 100 m, where 200 emitters characterized by $y=0.5$ and spacing of 0.50 m, was also considered (Case C). Friction losses were determined by using the Darcy–Weisbach–Blasius equations, whereas minor losses were determined as a function α of the kinetic head; simulations were carried out by considering α values equal to 0.0 (absence of local losses), 0.3, 0.6, 0.9, and 1.2.

The FSM procedure, starting from the upstream end toward the downstream end of the lateral, was used; the pressure head (H_{in}) and the total flow rate (Q_{in}) at the lateral inlet were initially assumed known. The computation procedure was iteratively repeated until the resulting inlet flow rate was equal to the total amount of water distributed by all the emitters. For each simulation, UC and DU were calculated by Eqs. (1a) and (1b).

Table 1 synthesizes, for each case and for the different α values, the initial flow rate, Q_{in} , the total and local losses along the lateral, H_f and H_L , respectively, as well as the values of the emission uniformity coefficients UC and DU. Values of the ratios H_f/H_{in} and H_L/H_{in} are also indicated. Table 1 shows that the friction and local losses obviously increase with

Table 1. Results of FSM Obtained for Different α Coefficients by Using Exponent y of $q(h)$ Relationship Equal to 0.5 (Case A) and 1.0 (Case B) and for Lateral Length of 100 m, with Emitter Spacing of 0.50 m (Case C)

α value	Q_{in} (L/h)	H_f (m)	H_f/H_{in} (ratio)	H_L (m)	H_L/H_{in} (ratio)	UC	DU
(a) Case A: $H_{in}=8.705$ m							
$\alpha=0.0$	303.3	1.95	0.22	0.00	0.00	0.969	0.983
$\alpha=0.3$	300.5	2.13	0.24	0.22	0.03	0.963	0.970
$\alpha=0.6$	397.7	2.30	0.26	0.42	0.05	0.957	0.957
$\alpha=0.9$	295.0	2.46	0.28	0.62	0.07	0.951	0.945
$\alpha=1.2$	292.4	2.61	0.30	0.81	0.09	0.944	0.933
(b) Case B: $H_{in}=8.568$ m							
$\alpha=0.0$	301.5	1.87	0.22	0.00	0.00	0.937	0.944
$\alpha=0.3$	296.9	2.01	0.24	0.21	0.02	0.928	0.924
$\alpha=0.6$	292.6	2.15	0.25	0.39	0.05	0.919	0.905
$\alpha=0.9$	288.5	2.27	0.27	0.57	0.07	0.909	0.888
$\alpha=1.2$	284.7	2.39	0.28	0.74	0.09	0.900	0.871
(c) Case C: $H_{in}=8.640$ m							
$\alpha=0.0$	398.9	2.05	0.24	0.00	0.00	0.951	0.975
$\alpha=0.3$	390.3	2.43	0.28	0.48	0.06	0.930	0.947
$\alpha=0.6$	382.4	2.77	0.32	0.91	0.11	0.909	0.922
$\alpha=0.9$	375.0	3.09	0.36	1.30	0.15	0.888	0.898
$\alpha=1.2$	368.1	3.37	0.39	1.65	0.19	0.867	0.875

increasing α ; consequently, the amount of the local losses, expressed as a function of the initial pressure head, give a result of 9% for the highest α value for Cases A and B and 19% for Case C.

Therefore, neglecting the local losses denotes the consequent overestimation of both the considered emission uniformity coefficients, whose values decrease with increasing α ; i.e., in Case A (lateral with 150 emitters), the DU resulting coefficient equal to 0.983 in the absence of local losses ($\alpha=0$), becomes 0.933 when α is 1.2. In Case C, because of the higher number of emitters installed along a shortened lateral (200 emitters in a 100 m length pipe), the influence of local losses becomes more relevant than in Cases A and B, as well as higher results in relative reduction of both the uniformity coefficients UC and DU.

Acknowledgments

The discussers wish to thank the Università degli Studi di Palermo for allowing cooperation with the Universidad Politécnica de Valencia. The discussers contributed equally on drawing up the discussion and in the final revision of the paper.

References

- Al Amoud, A. I. (1995). "Significance of energy losses due to emitter connections in trickle irrigation lines." *J. Agric. Eng. Res.*, 60(1), 1–5.
- Bagarello, V., and Pumo, D. (1992). "Lateral line hydraulics in drip irrigation systems." *Proc., 16th European Regional Conference of ICID*, Budapest, Hungary.
- Bagarello, V., Ferro, V., Provenzano, G. and Pumo, D. (1997). "Evaluating pressure losses in drip irrigation lines." *J. Irrig. Drain. Eng.*, 123(1), 1–7.
- Bralts, V. F., Barragan, J., and Wu, I. P. (1987). *Drip irrigation design and evaluating based on the statistical uniformity concept*, D. Hillel, ed., Vol. 4, Academic, New York, 67–117.
- Christiansen, J. E. (1942). "Irrigation by sprinkling." *California Agric. Exper. Station Bull. No. 670*, Univ. of California at Davis, Davis, Calif.
- De Marchi, G. (1954). "Idraulica." *Basi Scientifiche e applicazioni tecniche*, U. Hoeppli, ed., Milano. (in Italian).
- Howell, T. A., and Barinas, F. A. (1980). "Pressure losses across trickle irrigation fittings and emitters." *Trans. ASAE*, 23(4), 928–933.
- Jeppson, R. W. (1982). *Analysis of flow in pipe networks*, 5th Ed., Ann Arbor Science, Ann Arbor, Mich.
- Juana, L., Rodriguez-Sinobas, L., and Losada, A. (2002). "Determining minor head losses in drip irrigation laterals. I: Methodology." *J. Irrig. Drain. Eng.*, 128(6), 376–384.
- Palau-Salvador, G., Arviza Valverde, J., González-Altozano, P., Royuela Tomas, A., and Provenzano, G. (2004). "Evaluating pressure losses in drip irrigation laterals using computational fluid dynamic techniques (CFD)." *Proc., Euro AgEng Conf.*, Euro AgEng, Leuven, Belgium.
- Provenzano, G. (2004). "Discussion of 'Determining minor head losses in drip irrigation laterals. I: Methodology' by L. Juana, L. Rodriguez-Sinobas, and A. Losada." *J. Irrig. Drain. Eng.*, 130(3), 253–254.
- Provenzano, G., and Pumo, D., (2004). "Experimental analysis of local pressure losses for microirrigation laterals." *J. Irrig. Drain. Eng.*, 130(4), 318–324.
- Provenzano, G., Pumo, D., and Di Dio, P. (2004). "Simplified procedure to evaluate head losses in drip irrigation laterals." *J. Irrig. Drain. Eng.*, in press.
- Schlichting, H. (1980). *Boundary layer theory*, McGraw-Hill, New York.

- Valiantzas, J. D. (2002). "Continuous outflow variation along irrigation laterals: Effect of the number of outlets." *J. Irrig. Drain. Eng.*, 128(1), 34–42.
- Vallesquino, P., and Luque-Escamilla, P. L. (2002). "Equivalent friction factor method for hydraulic calculation in irrigation laterals." *J. Irrig. Drain. Eng.*, 128(5), 278–286.
- Veersteg, H. K., and Malalasekera, W. (1995). "An introduction to computational fluid dynamics." *The finite volume method*. Longman.
- Wu, I. P. (1997). "An assessment of hydraulic design of micro-irrigation systems." *Agric. Water Manage.* 32, 275–284.
- Zayani, K., Alouini, A., Lebdi, F., Lamaddalena, N. (2001). "Design of drip irrigation systems using the energy drop ratio approach." *Trans. ASAE*, 44(5), 1127–1133.

Closure to "Comparative Analysis of Hydraulic Calculation Methods in Design of Microirrigation Laterals" by Gürol Yıldırım and Necati Ağırlioğlu

May/June 2004, Vol. 130, No. 3, pp. 201–217.

DOI: 10.1061/(ASCE)0733-9437(2004)130:3(201)

Gürol Yıldırım¹ and Necati Ağırlioğlu²

¹Research Assistant, Civil Engineering Dept., Hydraulics Div., Istanbul Technical Univ., 34469, Maslak, Istanbul, Turkey. E-mail: yildirimg3@itu.edu.tr

²Professor, Civil Engineering Dept., Hydraulics Div., Istanbul Technical Univ., 34469, Maslak, Istanbul, Turkey. E-mail: necati@itu.edu.tr

The writers would like to express their appreciation to Provenzano and to Palau-Salvador for their interest in the original paper. The discussers have provided general clarification in relation to microirrigation lateral hydraulic problems. They emphasize the weight of local losses with respect to the total head-loss distribution along the pipeline. Moreover, to demonstrate that the modification of the flow streamlines induced local turbulence around the emitter, the velocity contours of three types of on-line emitters were also presented in the discussion in Figs. 1 and 2.

First, the original paper intended to present the state-of-the-art review of recent studies for microirrigation lateral design examined by the detailed comparison test for various combinations of the design parameters and for different uniform ground slope conditions, on the seven hydraulic calculation methods—the forward step method (FSM), the differential method (DM), the Runge-Kutta numerical method (RKM), the variable discharge method (VDM), the constant discharge method (CDM), the simplified analytical approach (SAA), and the successive approximations method (SAM)—taking into consideration the nonuniform outflow profile (except for the CDM method) along the lateral pipeline.

The comparison test shows that the computer-aided FSM (Hathoot et al. 1993) gives more precise results than those of the other six methods for all design cases because of the basic governing equations of the hydraulics of steady pipe flow. These basic governing equations are the Darcy-Weisbach friction formula, the continuity equation, and the conservation of energy equation coupled with the conservation of momentum equation. These equations are individually applied in each pipe segment between consecutive emitters, depending on the proper value of

the inlet pressure head determined by trial-and-error procedures, which can be applied by using a complex computer program. The main objective of this algorithm is to determine the proper value of the inlet pressure head. This value can be varied within limited design intervals on the basis of the initial and boundary conditions, as extensively discussed in the original paper.

In addition, the seven methods were analyzed and classified in Table 2 of the paper for comparative purposes from such points of view as solution methods, basic assumptions, formulations used, and differences in application. In this analysis, not one of these methods considers the effect of local losses in hydraulic computations.

Hathoot et al. (2000) also proposed a numerical approach that is an extension of the previous FSM method (Hathoot et al. 1993) for determining the effect of local pressure losses attributable to the various emitter barb sizes (small, medium, and large) on the energy losses in trickle irrigation laterals. According to these analyses, neglecting the effect of local losses may lead to design diameter errors of approximately 30% and errors in length of approximately 10%.

Provenzano and Pumo (2004) have presented an experimental investigation on the hydraulic analysis of local pressure losses in microirrigation laterals. This analysis deals with the hydraulic problem of evaluating local pressure losses attributable to insertions of integrated in-line or on-line emitters along the lateral line. That paper presents the numerical back-step calculation procedure, taking as its origin the lateral downstream closed-end section to verify the experimental results for determining local pressure losses in integrated in-line emitters. This procedure is similarly used in this discussion in the forward-step form, taking as the origin the lateral inlet section.

In the discussion, to determine the friction and local losses individually, some simple formulations [Eqs. (2) and (4)] are presented under the assumption of uniform emitter outflow. The validity of these formulations on the basis of this primitive assumption of uniform emitter outflow is limited because the actual energy-grade line of a lateral gradually decreases in the flow direction; therefore, the nonuniform outflow profile is actually evident along the lateral pipeline. The highest degree of accuracy provided by the FSM method cannot be reached by using this simplified procedure. Similar evaluations are also presented by the discussers, as clearly noticed in the discussion.

To show the practical value of these formulations, the computational example was presented in the "Numerical examples" section at the end of the discussion, and the results were shown in Table 1 of discussion. The section includes the following statement: "A computer spreadsheet that reproduces the procedure was devised by considering the data indicated in the discussed paper for determining inlet pressure head and by considering the emitters characterized by an exponent y equal to 0.5 (Case A) and equal to 1.0 (Case B). A lateral length of 100 m, where 200 emitters characterized by $y=0.5$ and spacing of 0.50 m was also considered (Case C). Friction losses were determined by using the Darcy-Weisbach-Blasius equations, whereas minor losses were determined as a function α of the kinetic head; simulations were carried out by considering α values equal to 0.0 (absence of local losses), 0.3, 0.6, 0.9, and 1.2."

Application

In the following, to better understand the discussers' computations and to clearly evaluate their corresponding clarifications, the numerical example presented in the section of the paper entitled

"To Determine Inlet Pressure Head" in accordance with Table 5 of the paper is resolved according to Eqs. (2) and (4) of the discussion for different values of the local loss coefficient, $\alpha=0.0, 0.3, 0.6, 0.9,$ and 1.2 ; and for the following three design cases: Case A ($H_{in}=8.705$ m $y=0.5$; $s=1.0$ m; $N=150$; $L=150$ m); Case B ($H_{in}=8.568$ m $y=1.0$; $s=1.0$ m; $N=150$; $L=150$ m); and Case C ($H_{in}=8.640$ m ($y=0.5$; $s=0.5$ m; $N=200$; $L=100$ m).

The commonly used data for the three design cases are given again: average outflow of the emitter, $q_{av}=2.0$ Lh⁻¹ ($5.555 \cdot 10^{-7}$ m³ s⁻¹); the corresponding average pressure head, $H_{av}=7.2$ m; the internal diameter and length of the lateral, $D=14$ mm and $L=150$ m; the ground slope, $s_0=0.0$; and the kinematic viscosity of irrigation water at 20°C, $\nu=1.01 \cdot 10^{-6}$ m² s⁻¹. The value of the coefficient k in Eq. (2) is taken to be 0.0246 for the Blasius friction coefficient formula, as reported in the discussion.

As explained in the discussion, the proposed forward-step computation procedure from the inlet (first emitter) toward the downstream closed end (Nth emitter) of the lateral was applied, assuming that the fixed values of the inlet pressure head for the three design cases are initially known; $H_{in}=8.705$ m (Case A), 8.568 m (Case B), and 8.640 m (Case C). The stepwise computation procedure was performed until the lateral inflow rate was equal to the total amount of emitter outflows, so the lateral inflow rate is an initially unknown parameter.

The numerical results obtained from this simplified procedure are shown in the Table 1 of this closure. In this table, for each of the design cases and for different values of α , the following are presented; values of the lateral inflow rate, Q_{in} ; downstream end pressure head at the Nth emitter, H_N ; total amount of friction losses, H_f ; total amount of local losses, H_l ; amount of total head losses, H_T , with their percentage values H_f/H_{in} , H_l/H_{in} , H_T/H_{in} ; as well as the values of the well-known uniformity coefficients UC and DU.

Results and Discussion

After comparing Table 1 of the discussion and Table 1 of the closure, some clarifications on the following unclear points are presented:

1. Principally, to maintain the steady flow conditions in a lateral, the sensitive balance between the inlet pressure head and the lateral inflow rate is obviously required (Yıldırım 2005). In other words, for an initially known value of the inlet pressure head, the value of the lateral inflow rate is an unknown variable and its value must be determined depending on the total amount of emitter outflows. According to Table 1 in the discussion, for the fixed initial values of the H_{in} and for the three design cases, the values of Q_{in} do not keep to the right the total amount of emitter outflows; this outcome would indicate that the sum of emitter outflows is greater than the values of Q_{in} , which means that backflow occurs from the downstream closed end toward the inlet upstream direction of the lateral. Similar evaluations were also presented by Yıldırım and Ağralıoğlu (2003, 2004).

As an exact solution, to get rid of the backflow in the pipe's downstream section, the greater values of Q_{in} were predetermined depending on the total amount of emitter outflows related to the fixed initial values of H_{in} , as given by Table 1 in this closure.

2. The section of the discussion related to this example includes, the following statement: "Table 1 synthesizes for each case and for the different α values the initial flow rate,

Table 1. Design Parameters According to Eqs. (2) and (4) in Discussion, for Different Values of Local Loss Coefficient (α) and for Three Design Cases A, B, and C

α	$Q_{in} \cong \sum_{i=1}^N q_i$ (Lh^{-1})	H_N (m) ^a	H_f (m)	H_l (m)	$H_T = H_f + H_l$ (m)	H_f/H_{in} (%)	H_l/H_{in} (%)	H_T/H_{in} (%)	$UC = 1 - \frac{1}{Nq_{av}} \sum_{i=1}^N q_i - q_{av} $ (%)	$DU = \frac{4}{\sum_{i=3N/4}^N q_{low,i}} Nq_{av}$ (%)
(a) Case A: $H_{in} = 8.705$ m ($y = 0.5$; $s = 1.0$ m; $N = 150$; $L = 150$ m)										
0.0	319.52	6.746	1.959	0.00	1.959	22.5	0.0	22.5	93.2	99.9
0.3	318.37	6.524	1.959	0.2218	2.181	22.5	2.5	25.0	93.3	99.9
0.6	317.21	6.302	1.959	0.4436	2.403	22.5	5.1	27.6	93.3	99.9
0.9	316.04	6.080	1.959	0.6654	2.624	22.5	7.6	30.1	93.2	98.9
1.2	314.86	5.858	1.959	0.8872	2.846	22.5	10.2	32.7	93.2	97.8
(b) Case B: $H_{in} = 8.568$ m ($y = 1.0$; $s = 1.0$ m; $N = 150$; $L = 150$ m)										
0.0	335.03	6.609	1.959	0.00	1.959	22.9	0.0	22.9	87.3	99.9
0.3	332.69	6.387	1.959	0.2218	2.181	22.9	2.6	25.5	87.4	98.9
0.6	330.36	6.165	1.959	0.4436	2.403	22.9	5.2	28.1	87.3	96.8
0.9	328.03	5.943	1.959	0.6654	2.624	22.9	7.8	30.7	87.2	94.6
1.2	325.69	5.721	1.959	0.8872	2.846	22.9	10.4	33.3	86.9	92.5
(c) Case C: $H_{in} = 8.640$ m ($y = 0.5$; $s = 0.5$ m; $N = 200$; $L = 100$ m)										
0.0	422.84	6.474	2.166	0.00	2.166	25.1	0.0	25.1	93.6	99.9
0.3	419.14	5.947	2.166	0.5271	2.693	25.1	6.1	31.2	93.5	98.7
0.6	415.35	5.419	2.166	1.0542	3.220	25.1	12.2	37.3	93.2	96.0
0.9	411.46	4.893	2.166	1.5813	3.747	25.1	18.3	43.4	92.7	93.3
1.2	407.47	4.366	2.166	2.1084	4.274	25.1	24.4	49.5	92.1	90.4

^aPressure head at the N th emitter located in the pipe downstream closed end.

Q_{in} , the total and local losses along the lateral, H_f and H_L , respectively, as well as the values of the emission uniformity coefficients UC and DU. Values of the ratios H_f/H_{in} and H_L/H_{in} are also indicated. Table 1 shows that the friction and local losses obviously increase with increasing α ; consequently, the amount of the local losses, expressed as a function of the initial pressure head, give a result of 9% for the highest α value for Cases A and B and 19% for Case C.”

From the above explanation, the notation H_f means the amount of “friction losses” but does not mean “total losses,” as confusingly written in the of the preceding statement. As indicated in the next sentence, the friction losses increase with increasing α , as also seen from Table 1 of the discussion.

For a one-fixed-emitter model, increasing the local loss coefficient only increases the amount of local losses (i.e., also increases the amount of total head losses) but it never changes the amount of friction losses.

As a matter of fact, as indicated in Eq. (2) of the discussion, the friction loss is a function of these unknown parameters: the average emitter outflow (or the emitter nominal flow rate) q_{av} , the pipe’s inside diameter D , and the emitter spacing S . In the computations shown in Table 1 of the discussion, the increasing friction losses for the three design cases may be attributed to using the variable data pairs (q_{av} and D) for each emitter model in accordance with the variable α values. Hence, these possible data sets for each emitter model should be provided in this discussion.

In line with this concept, for the one-emitter model selected in this example, Table 1 of this closure indicates that the friction losses yield the fixed values 1.959 m, 1.959 m, and 2.166 m for the Design Cases A, B, and C, respectively;

and the amount of local losses proportionally increase with increasing α (0.0, 0.3, 0.6, 0.9, and 1.2. for instance, for Design Cases A and B, $H_l = 0.0, 0.22, 0.44, 0.66,$ and 0.88 ; and for Design Case C, $H_l = 0.0, 0.527, 1.054, 1.581,$ and 2.108 . However, in the Table 1 of the discussion, the local losses do not proportionally increase with increasing α . For instance, for Design Case A, $H_L = 0.0, 0.22, 0.42, 0.62,$ and 0.81 ; for Design Case B: $H_L = 0.0, 0.21, 0.39, 0.57,$ and 0.74 ; and the Design Case C, $H_L = 0.0, 0.48, 0.91, 1.30,$ and 1.65 .

From Eq. (4) of the discussion, the local loss is a function of the same unknown parameters: q_{av} and D . Therefore, the values of the local loss may increase depending on the variable values of q_{av} and D , with increasing α . In other words, the data pairs (q_{av} and D) may be differently used for each emitter model in accordance with the increasing value of α . Therefore, the values of local loss may yield different values according to both tables. For instance, the amount of local losses, as a percentage of the inlet pressure head H_l/H_{in} , yields 10.2, 10.4, and 24.4%, in Table 1 of this closure; whereas it yields smaller values of 9, 9, and 19%, according to the Table 1 of the discussion for Design Cases A, B, and C, respectively.

- In Table 1 of this closure, increasing α has the effect of slightly changing the uniformity coefficient UC for Design Cases A and B, whereas decreasing both the uniformity coefficients is more significant for Design Case C than for the other two design cases, A and B.
- The lower-quarter distribution uniformity coefficient, DU, is defined as the average discharge for the lower-quarter segment of the lateral divided by the overall average q_{av} (Yitayew and Warrick 1988). To determine the actual value of this coefficient, the emitter outflows from the lower-

quarter segment of the lateral should be considered, as given by this form in the original paper (Table 3):

$$DU = \frac{4}{Nq_{av}} \sum_{i=3N/4}^{i=N} (q_{low})_i$$

However, Eq. (1b) of the discussion, for the interval of the integer i that represents the order of emitters, the following modification should be made:

$$\sum_{i=3N/4}^{i=N} (q_{low})_i$$

instead of

$$\sum_{i=1}^{i=N/4} (q_{low})_i$$

Errata

The following corrections should be made to the original paper:

- On page 210, in Fig. 2, the common x axis should read: "Reduced Inlet Pressure Head H_{in}/H_{av} "; and
- On page 206, the heading should include the shortened form: "Successive-Approximation Method (SAM)."

Acknowledgement

The writers thank the discussers and the other researchers whose methods are discussed in the paper, for their confirmations and opinions on the contents of the paper.

References

- Hathoot, H. M., Al-Amoud, A. I., Al-Mesned, A. S. (2000). "Design of trickle irrigation laterals considering emitter losses." *ICID J.*, 49(2), 1–14.
- Hathoot, H. M., Al-Amoud, A. I., Mohammad, F. S. (1993). "Analysis and design of trickle irrigation laterals." *J. Irrig. Drain. Eng.* 119(5), 756–767.
- Provenzano, G., and Pumo, D. (2004). "Experimental analysis of local pressure losses for microirrigation laterals." *J. Irrig. Drain. Eng.*, 130(4), 318–324.
- Yıldırım, G., (2005). "Analytical relationships for designing multiple outlets pipelines." *J. Irrig. Drain. Eng.*, in review.
- Yıldırım, G., and Ağralıoğlu, N. (2003). "Discussion of 'New algorithm for hydraulic calculation in irrigation laterals' by P. Vallesquino and P. L. Luque-Escamilla." *J. Irrig. Drain. Eng.*, 129(2), 142–144.
- Yıldırım, G., and Ağralıoğlu, N. (2004). "Discussion of 'Equivalent friction factor method for hydraulic calculation in irrigation laterals' by P. Vallesquino and P. L. Luque-Escamilla." *J. Irrig. Drain. Eng.*, 130(4), 335–339.
- Yitayew, M., and Warrick, A. W. (1988). "Trickle lateral hydraulics. II: Design and examples." *J. Irrig. Drain. Eng.*, 114(2), 289–300.

Discussion of "Determination of Length of a Horizontal Drain in Homogeneous Earth Dams" by Bhagu R. Chahar

November/December 2004, Vol. 130, No. 6, pp. 530–536.
DOI: 10.1061/(ASCE)0733-9437(2004)130:6(530)

Rajesh Srivastava¹

¹Associate Professor, Dept. of Civil Engineering, Indian Institute of Technology Kanpur, Kanpur 208016, India. E-mail: rajeshs@iitk.ac.in

The author has proposed simple equations for determining the length of drainage blanket and the downstream slope cover for a homogeneous earth dam. The discussor would like to mention the following points regarding the note:

1. Although the concepts are similar, the discussor believes that the use of a *vertical* downstream slope cover is preferable to *inclined* cover, as used by the author, especially since the "Discussion and Example" section mentions that the downstream slope cover should be more than the *height* of the capillary rise in soil forming the dam body.
2. The derivation of Eq. (11) may be presented in an alternative form as follows: The point on the parabolic phreatic line at which the slope is equal to $n:1$ is readily shown to be given by the coordinates $(-n^2a, 2na)$. The vertical downstream slope cover at this point is given by

$$d_v = \frac{l - a + n^2a}{n} - 2na = \frac{l - (1 + n^2)a}{n} \quad (1)$$

and the cover in the direction perpendicular to the downstream face is

$$d = \frac{nd_v}{\sqrt{1 + n^2}} = \frac{l}{\sqrt{1 + n^2}} - \frac{\sqrt{1 + n^2}}{2} (\sqrt{D^2 + h^2} - D) \quad (2)$$

3. The minimum effective length of the drain is obtained by assuming that $d=0$. Therefore, the meaning of the statement "minimum effective length of filter drain is independent of d " is not clear. If, for example, we assume that the minimum value of d depends on the capillary rise, l_{min} will be a function of d .
4. The concept of the maximum cover, as described in the note, appears to be unrealistic, since it is measured from an *imaginary* extension of the downstream face (Fig. 1 of the Technical Note) and since Eq. (26) is used to obtain l_{max} .

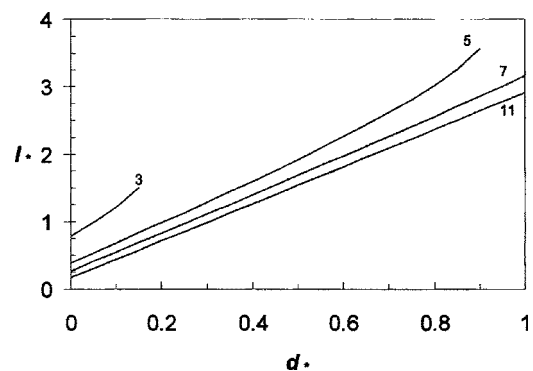


Fig. 1. Variation of filter length with downstream slope cover for $n=2.5$; numbers near curves represent value of b_*

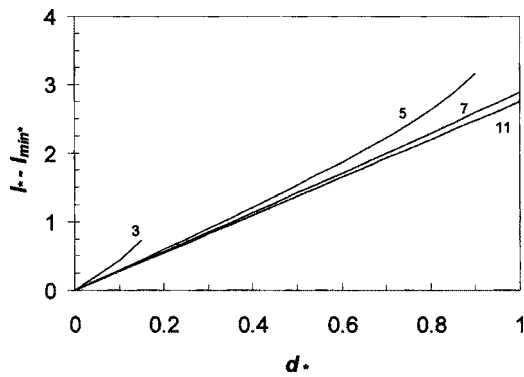


Fig. 2. Variation of additional filter length (over and above the minimum length) with downstream slope cover for $n=2.5$; numbers near curves represent value of b_*

The discussor believes that the author's procedure will work only when the perpendicular from point f' intersects the downstream face (and not its extension). For instance, in the example considered by the author, if we increase the drain length to 50 m, we find that $d=10.7$ m. A plot of the basic parabola and the correction near the upstream face shows that this value of d is indeed correct and is greater than the d_{max} proposed by the author (8.4 m). Therefore, if the cover is considered perpendicular to the downstream face, finding l_{max} is a little more complicated than the procedure suggested by the author. The author may want to attempt it, although the discussor believes that the utility of the maximum cover concept is rather limited and that Eq. (4) given subsequently should be reasonably good (although probably on the higher side).

If vertical cover is considered, the discussor believes that d_{max} should be based on the limiting condition when the vertex of the Kozeny's parabola is vertically below the point d' in Fig. 1 of the Technical Note. The vertical downstream slope cover is then equal to the height of the dam, $h+F_B$ (further increase in the length of the drain would not increase the vertical downstream slope cover), and the length of the drain is given by

$$l_{max} = n(h + F_B) + a = n(h + F_B) + \frac{\sqrt{D^2 + h^2} - D}{2} \quad (3)$$

which may be solved to obtain

$$l_{max} = n(h + F_B) + \frac{h^2}{4(T + mF_B + 0.3mh)} \quad (4)$$

- Defining $b_* = 0.3m + n + F_B(m + n) + T_*$, Figs. 2(a, c, and d) of the Technical Note can be presented concisely in a single figure, as shown in Fig. 1 here. Although the linear relationship between l_* and d_* is apparent for larger values of b_* , the same does not hold true for smaller values. As the author states, this range may be outside the practical range, and the assumption of linearity should be satisfactory in most cases. However, from the statement after Eq. (37) of the Technical Note that "the length of the filter more than minimum length is not affected by m , F_B , and T for a specified n and d' "

appears to be based on Fig. 2, which is exact and not Eq. (37), which is approximate. A plot of $l-l_{min}$, as in Fig. 2 of this discussion, indicates that it is only approximately correct and that too at large values of b_* .

The discussor believes that incorporating these comments can enhance the useful contribution by the author.

Closure to "Determination of Length of a Horizontal Drain in Homogeneous Earth Dams" by Bhagu R. Chahar

November/December 2004, Vol. 130, No. 6, pp. 530-536.

DOI: 10.1061/(ASCE)0733-9437(2004)130:6(530)

Bhagu R. Chahar¹

¹Assistant Professor, Dept. of Civil Engineering, Indian Institute of Technology Delhi, Hauz Khas, New Delhi-110 016, India. E-mail: chahar@civil.iitd.ac.in; Chahar_br@yahoo.com (alternate).

The writer thanks the discussor for his interest in the article. In response to the comments of the discussor, the writer has the following observations. Safeguarding against the capillary rise a vertical downstream slope cover (d_v) is preferable, as pointed out by the discussor and as also used by Mishra and Singh (2005). The cover normal to the downstream face (d) is more general, since the vertical cover is a special case given by

$$d_v = \frac{\sqrt{1+n^2}}{n}d \quad (1)$$

until the point of tangency ($-n^2a, 2na$) is downstream of the point d' . If it is upstream of d' , i.e.,

$$n^2a > n(F_B + h) + a - l \quad (2)$$

then

$$d_v = \frac{\sqrt{1+n^2}}{n}d - \left(na - F_B - h + \frac{l-a}{n} \right) = F_B + h - 2na \quad (3)$$

Therefore, the reverse relation of d from d_v , as given in Eq. (2) of the discussion is not valid in the range given by Eq. (3).

The minimum effective length of the drain (l_{min}) was defined as the length that keeps the phreatic line just within the body of the dam or, in other words, as the length at which the phreatic line tends to intersect the downstream face. This condition is attained when $d=0$ and capillarity is neglected, so l_{min} was said to be independent of d . If the minimum cover (d_{min} or $d_{v\ min}$) is provided considering the effect of the capillary rise, then l_{min} will be a function of d_{min} or $d_{v\ min}$.

The writer still believes that the proposed concept for d_{max} and l_{max} is all right. For a given dam geometry (m , n , T , and $h+F_B$), the point of tangency ($-n^2a, 2na$) shifts upstream as l or d (consequently a) is increased. In fact, the controlling parameter is the $h/(B-l)$ ratio. The vertical cover increases with the increase in this ratio and attains maximum value ($d_{v\ max}$) when the point of tangency (not the vertex of the parabola, as mentioned by the discussor) is vertically below the point d' . Therefore, $d_{v\ max} = h + F_B - 2na$ instead of $d_{v\ max} = h + F_B$. With a further increase in the $h/(B-l)$ ratio, the value of d_v decreases, although the value of d keeps on increasing. Moreover, with an increase in the $h/(B-l)$ ratio, the inflection point on the phreatic line also shifts toward the point f' ; and for

large values, it vanishes, i.e., the points g' and f' coincide (Polubarinova-Kochina 1962). Thus for a large $h/(B-l)$ ratio, the point of tangency can shift up to the point f' , resulting in the maximum cover normal to the downstream face as d_{\max} , obtained in Eq. (19). Accordingly, d_{\max} can safely be estimated by using Eq. (29).

Although Fig. 1 of the discussor is concise, it conceals the dependencies of l and d on the dam geometry, whereas Figs. 2(a, c, and d) of the Technical Note reveal such information. Figs. 1 and 2 of the discussor have been plotted for the range of d_* up to 1.0, but in practice d_{\max}^* (except for very large F_{B^*}) seldom exceeds 0.5. The linear relationship between l_* and d_* is more apparent in this range. A person who is interested in a parameter such as b_* should prefer a , which has physical significance. Actually a is the portion of the drainage blanket that acts as a filter, which requires careful designing. However, the remaining portion ($l-a$) acts as a drain to intercepted water by the filtered portion, which could even be a pipe drain or coarse dumped material. Combining Eq. (14) into Eq. (2)

$$a_* = \frac{\sqrt{(0.3m+n+F_{B^*}(m+n)+T_*-l_*)^2+1} - (0.3m+n+F_{B^*}(m+n)+T_*-l_*)}{2} \quad (4)$$

where $a_*=a/h$. Using Eqs. (17) of the Technical Note and Eq. (4) of this closure

$$l_* = \sqrt{1+n^2}d_* + (1+n^2)a_* \quad (5)$$

Eq. (5) indicates that plots between l_* and d_* are straight lines for a fixed value of a_* with slopes $(1+n^2)^{1/2}$ and intercepts $(1+n^2)a_*$ similar to Fig. 2(b) of the Technical Note; whereas for a fixed value of n , the plots will be parallel straight lines replacing Figs. 2(a, c, and d). However, Eq. (5) has a limitation in that the relationship is implicit, since a is also a function of l .

References

- Mishra, G. C., and Singh, A. K. (2005). "Seepage through a levee." *Int. J. Geomech.*, 5(1), 74–79.
- Polubarinova-Kochina, P. Ya. (1962). *Theory of ground water movement*, Princeton University Press, Princeton, N.J.